Advances in Science and Technology Research Journal

Advances in Science and Technology Research Journal 2023, 17(6), 254–273
https://doi.org/10.12913/22998624/174970
ISSN 2299-8624, License CC-BY 4.0

Received: 2023.09.06
Accepted: 2023.11.08
Published: 2023.11.21

Study on Near-Dry EDM Performance Characteristics of MSGNP/Al-7075 Using Air, Argon, Nitrogen, and Freon Dielectric Medium

Haneen Lateef Abd[1*], Saad Mahmood Ali[2]

[1] Production Engineering and Metallurgy Department, University of Technology, Iraq, Baghdad, Iraq
[2] Biomedical Engineering Department, University of Technology, Iraq, Baghdad, Iraq
* Corresponding author's e-mail: haneenlateef92@gmail.com

ABSTRACT

The primary aim of the current study is to investigate the influence of input parameters of near dry electric discharge machine (ND-EDM) upon the output performances including the MRR, EWR, SR and WLT for the fabricated new metal matrix composite (MMCs) of aluminum A7075 matrix nanocomposites by adding 8% of Microscopic Slide Glass Nanoparticles (MSGNPs) as reinforcements to improve the metallurgical and mechanical properties of Al-7075/MSGNP composites using stir-casting method. In ND-EDM the dielectric medium plays a significant role in the procedure responses. In the current work, the vegetable oil with gases, such as air, Ar, mix (Ar+N_2), and Freon were used as a dielectric media. The obtained results show that the highest MRR achieved when using the vegetable oil + Freon gas, reached 29.425 mm^3/min, and then 26.943 mm^3/min when using the vegetable oil + Air as a dielectric. The lowest EWR achieved when employing the vegetable oil + Argon gas, reached 0.120 mm^3/min, and then 0.175 mm^3/min. The lowest SR values obtained for all the designed experiments reached 3.287 µm when using Ip (10 A), Ton (1600 µsec), and Ar additive gas, followed by 4.567 µm when adding Freon gases to the dielectric. In the ND-EDM, the average of recast white layer thickness in the case of vegetable oil + air, vegetable oil + Ar, vegetable oil + mix (Ar-N_2), and vegetable oil + Freon was 1.505, 1.180, 0.456, and 0 µm, respectively. These unique results can be used to increase the service and fatigue life of parts and machines that are exposed to sudden dynamic mechanical or thermal loads, without the need for additional operations to remove this brittle layer, which causes the failure of these parts with a short service life. The created mathematical models displayed a higher value of R-Square and the adjusted R-square, which manifest a better fit. Normal probability plots of the residuals for MRR, EWR, and SR elucidated an obvious pattern (i.e., the points were stabilized in a straight line) which indicates that every factor affects the mentioned responses and the outcomes of these responses from the regression model (predicted value by factorial) and the true values (from the experiments).

Keywords: surface roughness, material removal rate, nitrogen, metal matrix composite, electrode were ratio, white layer thickness, argon

INTRODUCTION

The EDM method has become an essential tool of production applications, including die-making, medicinal, aerospace and power generation, and precision machining. Unlimited material hardness is one of the major advantages over traditional manufacturing techniques, as it allows for the processing of complicated geometries in difficult-to-machine materials [1]. Furthermore, because there is no contact between the electrode and the workpiece in EDM, the mechanical stress, chatter, and vibration problems are avoided during the processing. The development of computer helped solve many mathematical modeling issues associated with EDM processes, which led to a notable improvement in EDM. In the past 50 years, EDM has undergone significant advancements and development, including the introduction of Wire-cut Electrical Discharge Machining (W-EDM), micro EDM, dry EDM machining, powder-mixed EDM, and

ultrasonic-assisted EDM**,** which contribute the performance enhancement [2-4].

By creating a series of brief electrical discharges between the tool electrode and the workpiece while immersing both in a dielectric fluid, EDM is a thermo-electrical technique for removing material. The material removal mechanism is a complex process that involves many physical processes [5-6]. Material Removal Rate (MRR), Electrode Wear Rate (EWR), Total Wear Ratio (TWR), and Surface Finish (SR) are all metrics used to evaluate the EDM performance and are modified by the electrode, dielectric, and workpiece material [5]. Machinability in the EDM is depended upon the electric conductivity rather than the mechanical qualities. The performance of EDM is influenced by the dielectric fluid and in turn, EDM affects the environment [7]. The type of dielectric used during machining has a significant impact on the process. Employing gases or air as a dielectric fluid has a significant influence upon the procedure of machining [8-10]. Nevertheless, EDM possesses an important ecological influence because, through the procedure of machining, poisonous emissions are generated owing to the high temperature produced. The heavy as well as poorly bio-degradable substances are blended in the slurry, and the emission of electromagnetic radiation will hurt the environment [11-12].

The environmental concerns associated with the process have been a major drawback of EDM. EDM in hydrocarbon oils may result in problems, such as the creation of hazardous gases (CO and CH_4), aerosols, and odors. As strong skin irritants, these oils can cause contact dermatitis when exposed over an extended period [13-14]. Other EDM variants have been researched because of the environmental issues, scarcity of petroleum products, rising hydrocarbon oil prices, fire dangers, and odor of burning, and a need to increase the process' productivity [15-16]. The Near-Dry EDM (ND-EDM) and Dry EDM are environmentally friendly versions of the processes of EDM [17].

Recent developments have highlighted the need for Metal Matrix Composites (MMCs) as they are a common material for structural, corrosion, thermal, transportation, electrical, automotive, and aerospace applications, such as cylinder liners, engine pistons, and disc brakes, so they continue to be developed as they have many benefits, including the ratio of high strength to weight, toughness, and resistance to wear [18-20]. However, due to the material's brittleness and hardness, producing composite wafers is problematic [21]. This characteristic, combined with the material's expensive cost, necessitates research to enhance the production process and, as a result, enable the widespread use of composite-based products [22-24]. The main objectives of the present research include examining the effects of ND-EDM input process parameters, including the current (Ip), pulse on time (Ton), and type of dielectric using a gaseous mixture, such as air, argon, mixed (argon + nitrogen), and Freon with vegetable oil on the surface integrity for fabricated metal matrix composites (MMCs) as a workpiece to forecast the optimum levels of input process parameters.

MATERIALS AND METHODOLOGY

In this work, the metal matrix composites (MMCs) workpieces contain Aluminum alloy (Al7075) matrix, which is an important material in the automotive and aerospace industries, such as cylinder liners, engine pistons, brake discs, etc., as the matrix materials, while the reinforcement materials are the Microscopic Slide Glass Nanoparticles (MSGNPs). Development of these composite materials has many benefits, including high hardness, strong strength-to-weight ratio, and corrosion resistance [25].

The Al alloy (Al7075) was utilized as a matrix material since it's a precipitation-hardened Al alloy with Zn, Mg, Cu, and Cr as the chief alloying components. It has good mechanical properties, as it has a good strength value comparable to many steels. It also has good fatigue strength and high corrosion resistance, among other similar alloys. Tables 1 and 2 show the chemical composition and mechanical properties of the used alloy ingot imported and examined by Hanwei Company, Chain. The purchased ingot plate has dimensions (500 x 200 mm) and a thickness (2 mm). The plate was cut into small strips to be put in a suitable melting pot for stir casting.

The glass powder was utilized as the main strengthening material in the nanoparticles form determined from the microscopic slides. The sieved fine glass powder has a 35 nm size. The chemical composition of particles, size of particle, thermal, physical, and mechanical properties

Table 1. The chemical composition of Al7075 aluminum alloy (wt.%)

Element	Mg	Fe	Ti	Si	Mn	Zn	Cu	Ti	Cr	Al
Wt.% composition	2.5	0.5	0.02	0.4	0.3	5.6	1.5	0.2	0.15	Balance

Table 2. The mechanical properties of Al 7075

Item	Unit	Values
Density	g/cc	2.81
Hardness (HB 500)		30
Compressive strength	MPa	330
Ultimatetensile strength	MPa	200
Elongation	%	11
Modulus of elasticity	GPa	71.7
Poisson's ratio		0.33
Machinability	%	70
Melting temperature	°C	677-700
Shear modulus	GPa	26.9
Shear strength	MPa	331

of the MSGNPs tests were carried out in the Ministry of Science and Technology laboratories.

The proposed metal matrix composite was fabricated by using also a different composition varied from 0 to 10% wt of MSGNP, where the amount of magnesium is kept to be constant at 2%. Besides that flux 1 wt.% was added for removing the slug. The process of stir casting is the simplest and least expensive method of making AMCs. The significant topic in such method is getting a virtuous wetting between the particle reinforcement and the melted metal, to ensure a more uniform dispersion of the reinforcing particles [26].

The fabricated workpiece composites were examined by using scanning electron microscope (SEM) and X-Ray Diffraction (XRD) analysis. The XRD test of workpiece materials was performed employing the technique of backloading preparation [27]. The tensile test was conducted according to standard (ASTM-E8) at the room temperature utilizing a universal tensile testing machine (WDW-200E) with a 20 kN exerted load and a 0.5 mm/min strain rate. Hardness test specimens were prepared using the Rockwell hardness test according to standard (ASTM E-18). The samples' smooth surfaces were indented for a dwell time of 10 sec using a load of 100 kg.

The chemical composition for fabrication workpiece materials Al 7075/MSGNP comprises Al, Mg, Fe, and silica, and the latter of which is augmented via adding the nanoparticles of glass for improving the tensile strength, hardness, higher corrosion, and resistance to rupture at the high-temperature conditions. In addition, the produced workpiece contains other elements, such as nickel, manganese, zinc, copper, and caladium. There is a significant chemical reaction between MSGNP and aluminum particles.

The microstructural characterization of the composites of Al7075 alloy at 8 wt.% nano clear glass powder revealed a virtuous metallurgical bonding among the particles of aluminum. The Scanning Electron Microscope (SEM) images and Energy Dispersive X-ray Spectroscopy (EDX) patterns of Al 7075/MSGNP analysis were performed for examining the adsorption of glass in the matrix of Al and any else elements that might be existing between the matrixes. The analysis of EDX demonstrates that the presence of the composition of silicon increases into the composites compared with the base alloy. The alloying components of the base alloy (Al7075) matrix are denoted via the O, Na and C peaks. The outcomes of the study of EDX for the whole Al7075/MSGNP compositions were to work as example for oxidation as well as SiO_2 existence; therefore it was chosen the 8% workpiece composition in the present work. Table 3 depicts the chemical composition of Al 7075/MSGNP that was listed per EDX.

By reviewing the results of the mechanical tests that were conducted, it showed that for the manufacture of Al7075 matrix for workpieces with glass nanoparticles at a weight ratio of 8 wt.% MSGNP, the hardness and tensile strength

Table 3. The chemical composition of Al 7075/MSGNP via EDX

Element	Wt.% composition	Element	Wt.% composition
Mg	1.12	Ni	0.01
Fe	0.22	Ti	0.02
Si	1.83	Na	2.1
Cu	1.37	C	0.02
Mn	0.14	O	0.01
Zn	5.84	Al	Balance

were increased and reached the maximum values. The Al7075 alloy's microstructure analysis also revealed a virtuous metallic bonding among the particles of aluminum, and the uniformly dispersed and transparent glass particles at the optimal addition of 8 wt.%. From the aforementioned, it can be concluded that the best manufactured and evaluated alloy is Al7075/MSGNP with 8 wt.%. Therefore, a decision was made to adopt it as the workpiece material throughout the following investigational process of the current work.

In the present work, the hybrid setup of near-dry (ND-EDM) was developed indigenously by manufacturing and preparing the required attachments locally as one of the contributions of the work, where an additional attachment was utilized to supply a two-phase (liquid, and gas) dielectric medium between tool and workpiece, as shown in Figure 1. The system unit consisted of a gas cylinder, an air compressor, a gas filter, a milling vise for placing the workpiece, a dielectric fluid tank, a pump to recycle the dielectric fluid, mist unit, several flexible tubes for passage of high-pressurized dielectric medium, a tool holder and filters to clean the dielectric fluid between them. Compressed air and gas were provided by the air compressor and gas cylinder, respectively. The tank was filled with an appropriate level of dielectric medium (vegetable oil). Also, the setup unit comprises the gauges of air and gas pressure that obtain the operating dielectric gas pressure, with a range between 0.1 MPa to 0.5 MPa. The experiments were conducted upon a Die-sinking EDM (machine Model CHMER, CM 323C), located in the Training and Workshops Center/University of Technology. In such setup, a metal matrix composite workpiece was used as an anode, and a Cu electrode material was used as a cathode.

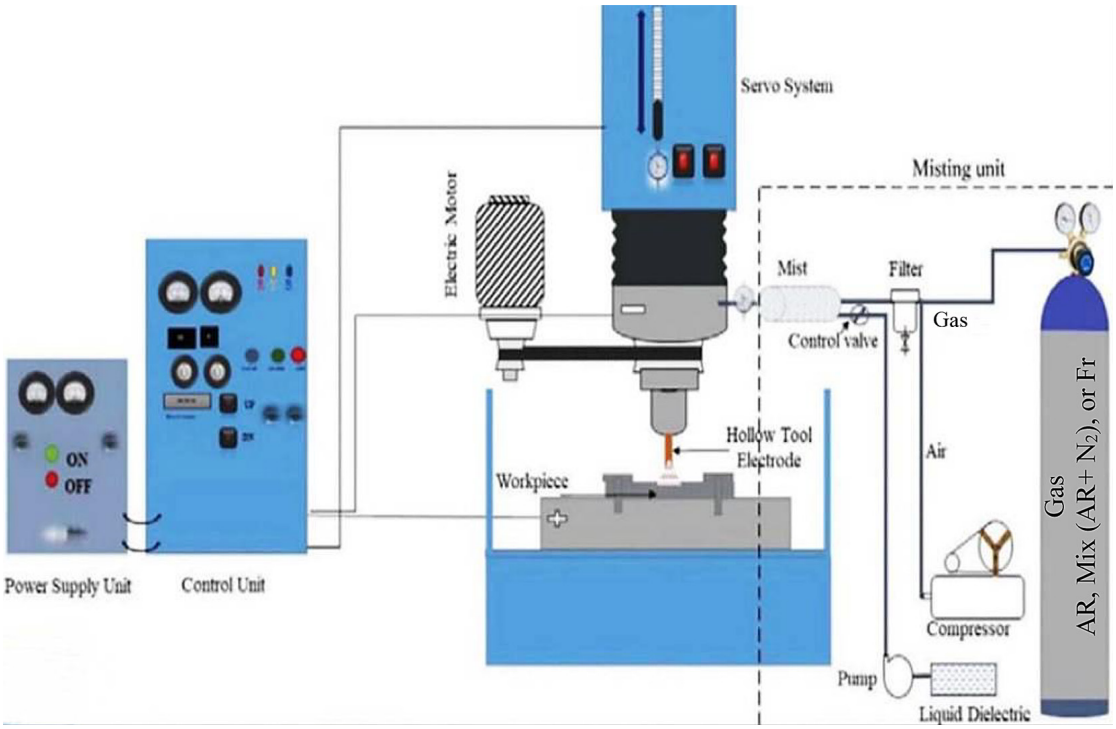

Fig. 1. The schematic of the ND-EDM process used in a die sinking EDM machine

Table 4. The designed parameters of process for the Near Dry-EDM experimentation

Process parameter	Unit	ND-EDM
Dielectric medium		Vegetable oil + [air, argon, mix (argon+ nitrogen), and freon]
Machining time	Sec	0.2
Discharge current	A	10, 24, 50
Pulse on	µs	800, 1600
Pulse off	µs	800
Gap voltage	V	10
High voltage		140
Low voltage	A	30
Working pressure	MPa	0.1–0.5
Jumping time	m/min.	0.4
· Workpiece electrode – metal matrix composite, Tool electrode – Copper		

The schematic of the ND-EDM process with the developed experimental facility is shown in the Figure 1. The parameters of process for the ND-EDM and WET-EDM experimentation are given in the Table 4.

This work explores choosing the best machining parameters by using the WET-EDM and ND-EDM setup, including the workpiece manufacturing techniques, its metallurgical characterization and mechanical properties, and the electrode design, to achieve the best measurement of the output performance parameters, comprising the Material Removal Rate (MRR), Electrode Wear Ratio (EWR), Surface roughness (SR), and White Layer Thickness (WLT).

The dielectric fluid used in the EDM process possesses an important influence upon the productivity, cost, and machined parts quality. Concerns for safety, environment, and health must all be taken into consideration. In the experiments of the present work, an attempt was made to machine a metal matrix composite workpiece by using different methods and types of dielectric medium. The physical properties of the vegetable oil, air, argon, mix (Argon+Nitrogen), and Freon as dielectric materials are listed in Table 5. Other constant selected machining parameters, including S code (200), machining time (0.2 s), pulse off time (Poff) (800 µs), gap voltage (10 V), high voltage (140 V), low voltage (30 V), working pressure (0.1-0.5 MPa), jumping time (0.4 mm), and dielectric gas flow rate (ml/min).

In the current EDM processes, the electrode is the tool that specifies the shape of the hollow shaft that has been produced. The electrode material must satisfy some criteria, including it must be useable, have a corrosion and thermal resistance, be electrically conductive, offer excellent surface finishing, resist thermal damage, the ability to machine with a higher material removal rate, lower tool wear ratio, machinability, and availability at low cost. The polarity, frequency, and density of the electrodes are the key determinants of wear rates. EDM electrodes are commonly made of several types of graphite, copper, tungsten, brass, silver, and steel. Every material has unique characteristics that make it more suitable for some uses than others. A hollow copper instrument with an internal cleaning system was used in this experimental work. The used tool material was copper (99.96%) purity, with length of (55 mm), and 6 and 12 mm inner and outer diameter, correspondingly. Cu was chosen as a tool substance due to its less price, elevated thermal

Table 5. The physical properties of dielectric fluids

Dielectric	Density (kg/m^3)	Viscosity (kg/m.s)	Thermal conductivity (W/m.K)	Specific heat (J/kg.K)
Air	1.229	1.647×10^{-5}	0.026	1006
Argon	1.622	2.125×10^{-5}	0.015	520.64
Nitrogen	1.138	1.663×10^{-5}	0.024	1040.67
Freon	3.220	2.791×10^{-5}	0.109	840.20
Vegetable oil	919.21	4.021×10^{-5}	0.16	2171

Table 6. The Cu electrode chemical analysis

Element	%Zn	%Pb	%Sn	%P	%Mn	%Fe	%Ni	%Si	%Cr
Weight %	0.0001	0.0005	0.0005	0.0001	0.0002	0.0091	0.0004	0.0373	0.0008
Element	%Al	%S	%As	%Ag	%Co	%Bi	%Cd	%Sb	%Cu
Weight %	0.0024	0.0001	0.0001	0.0024	0.0004	0.0001	0.0001	0.0017	Resides

Table 7. The physical and Mechanical properties of the copper electrode

Physical and mechanical properties	Values	Physical and mechanical properties	Values
Electrical conductivity (S/m)	58.5	Density (g/cm³)	8.94
Thermal conductivity at 20 °C in (W/m.°C)	18	Tensile strength (MPa)	62.0
Electrical resistivity at 20 °C in (Ω mm²/m)	0.017	Elongation (%)	7
Modulus of elasticity in (GPa)	115	Yield strength (MPa)	57.9
Coefficient of thermal expansion in (ppm/°C)	17.7	Hardness, HRB	62
Melting point (°C)	1083		

and electrical conductivity, and ease of production. Before machining, a specimen of the used electrode copper was tested at the Central Organization for Standards and Quality Control in Baghdad to analyze the chemical composition as well as the physical and mechanical properties. Their results are displayed in Tables 6 and 7.

The Design of Experiments (DOE) is essential in determining the required number of experiments. It involves two parameters and two levels for Near-EDM experiments. For each dielectric individually, the effects of the pulse-on-time and current parameters on the MRR, EWR, SR, and WLT were investigated. The metal matrix composite workpiece was considered an anode, while the copper electrode was regarded to be the cathode electrode. The workpiece (AMC) dimensions of (40 x 30 x 100 mm) were cut by using a wire-EDM machine into small workpiece dimensions of (40 x 30 x 1 mm). For the implementation of experiments, tubular copper tool electrodes with outer and inner diameters of 12 and 6 mm, respectively were fabricated. Before each experiment, the electrode end is polished with a fine abrasive paper. The electrode and workpiece were cleaned from the impurities before recording their weights. The workpiece and electrode were weighed by using a digital balance before and after the EDM processes. The electrode was placed into the tool holder, which creates the cathode terminal, and an indicator gauge was used to confirm the electrode's centricity. To generate the hole cavity on the upper surface of the workpiece in each experiment, an electrode with a 6 mm diameter and 0.5 mm depth was employed.

After each machining operation, the workpiece and electrode was cleaned and dried to be free from the dielectric material, debris or dirt. The weighing process was done by using a precision electronic balance (Type Denver instrument, 4 digits) with a (0.0001-210 gm) measuring range and (0.0001 gm) accuracy. MRR, which is based upon the weight of workpiece prior and beyond the process of machining as well as the anticipated time of machining, was computed. EWR is a significant parameter since it influences the dimensional accuracy of workpiece. The equation indicates that the EWR was stated as the discrepancy between the weight of electrode prior and beyond the process of machining and the time of machining.

The surface roughness (SR) of three different sections of the machined surface was measured. The average of these three measurements was used to calculate the final surface roughness value, which was represented in μm. The Pocket Surf PS1 profilometer was utilized for measure the surface roughness (SR) at Maher General Company. In this device, a probe scans the surface and contrasts the peaks as well as the troughs for locating the surface roughness (SR). The probe direction of the through the trace was visible on a digital screen. To measure the white layer thickness (WLT), the workpiece samples were prepared for scanning electron microscopy. The samples were subjected to a diversity of mounting, grinding, polishing, and gold coating techniques. These examinations were conducted in the metallurgical processing and metallurgical testing laboratories of the Department of Production and Metallurgy Engineering/University of

Technology. To determine the white layer thickness, the machining surfaces of the Al7075/MS-GNP composite were examined by using the FE-Scan electron microscopy.

RESULTS AND DISCUSSIONS

The outcomes were determined beyond the Near-EDM process in the experimental work. These results were utilized for developing a mathematical model for predicting different response characteristics via employing Minitab 18 software and then analyzing the predicted outcomes and comparing them with the experimental values. As well, Analyses of Variance (ANOVA) were utilized for defining the highly effective input factors to every response in the procedure. Full factorial designed experiments were performed for experiments, including four experimental groups of ND-EDM methods. Tables (8 to 11) show the response performance results that were analyzed by using the full factorial design (FFD) approach and the Minitab 18 software as discussed below for MRR, EWR, SR with the input parameters of the ND-EDM results of the experiments when using the vegetable oil with a gas, such as air, Ar, mix ($Ar+N_2$), and Freon, respectively.

The results analysis manifested that both the current and the pulse on time were significant process parameters for MRR in ND-EDM. In Figure 2 (a to d), the MRR increased with increasing the used current from 10 A to 30 A by 507.94% and 613.35% using vegetable oil + Air dielectric, 865.16% and 249.11% using vegetable oil + Ar, 444.52% and 1013.14% using vegetable

Table 8. The response performance results for ND-EDM (Vegetable oil + Air)

No.	Ip Amp	Ton µsec	MRR g/min	MRR mm^3/min	EWR g/min	EWR mm^3/mm	SR µm
1	10	800	$9.176*10^{-3}$	3.301	$9.647*10^{-3}$	1.079	5.117
2	10	1600	0.0105	3.777	$8.609*10^{-3}$	0.972	5.297
3	30	800	0.0556	20.068	$3.092*10^{-3}$	0.346	5.311
4	30	1600	0.0749	26.943	$4.059*10^{-3}$	0.454	5.352

Table 9. The response performance results for ND-EDM (Vegetable oil + Ar)

No.	Ip Amp	Ton µsec	MRR g/min	MRR mm^3/min	EWR g/min	EWR mm^3/min	SR µm
1	10	800	$4.062*10^{-3}$	1.461	$1.068*10^{-3}$	0.120	4.761
2	10	1600	$7.160*10^{-3}$	2.576	$4.022*10^{-3}$	0.450	5.287
3	30	800	0.0392	14.101	$3.75*10^{-3}$	0.420	5.937
4	30	1600	0.025	8.993	$9.677*10^{-3}$	1.082	6.276

Table 10. The response performance results for ND-EDM (Vegetable oil + mix ($Ar+N_2$))

No.	Ip Amp	Ton µsec	MRR g/min	MRR mm^3/min	EWR g/min	EWR mm^3/min	SR µm
1	10	800	$9*10^{-3}$	3.237	$1*10^{-4}$	1.119	3.814
2	10	1600	$4.130*10^{-3}$	1.486	$1.304*10^{-4}$	1.459	5.561
3	30	800	0.049	17.626	$3.703*10^{-4}$	4.142	6.012
4	30	1600	0.046	16.547	$2.2*10^{-4}$	2.461	6.812

Table 11. The response performance results for ND-EDM (Vegetable oil + Freon gas)

No.	Ip Amp	Ton µsec	MRR g/min	MRR mm^3/min	EWR g/min	EWR mm^3/min	SR µm
1	10	800	$8.137*10^{-3}$	2.927	$2.712*10^{-3}$	0.303	4.567
2	10	1600	$8.7*10^{-3}$	3.130	$2.3*10^{-3}$	0.257	4.634
3	30	800	0.0556	20.000	$1.568*10^{-3}$	0.175	5.461
4	30	1600	0.0818	29.425	$6.9767*10^{-3}$	0.780	6.341

oil + mix (Ar+N_2, and 583.29% and 840.10% using vegetable oil + Freon gas, when the utilized pulse-on-time values were 800 µs and 1600 µs, respectively. Figure 3 (a to d) elucidates that the MRR slightly increased or decreased with increasing the used T_{on} from 800 µs to 1600 µs by 14.42% and 34.26% using vegetable oil + Air dielectric, 75.70% and -56.80 % (reduction) using ND-EDM (Vegetable oil + Ar), -117.84% (reduction) and -6.52% (reduction) using vegetable oil + mix (Ar+N_2), and 10.32% and 47.13% using vegetable oil + Freon gas), when the utilized pulse current values were 10 A and 30 A, respectively. The MRR increases rapidly when the pulse current increases. As the current was raised, the discharge power per pulse augmented, which further

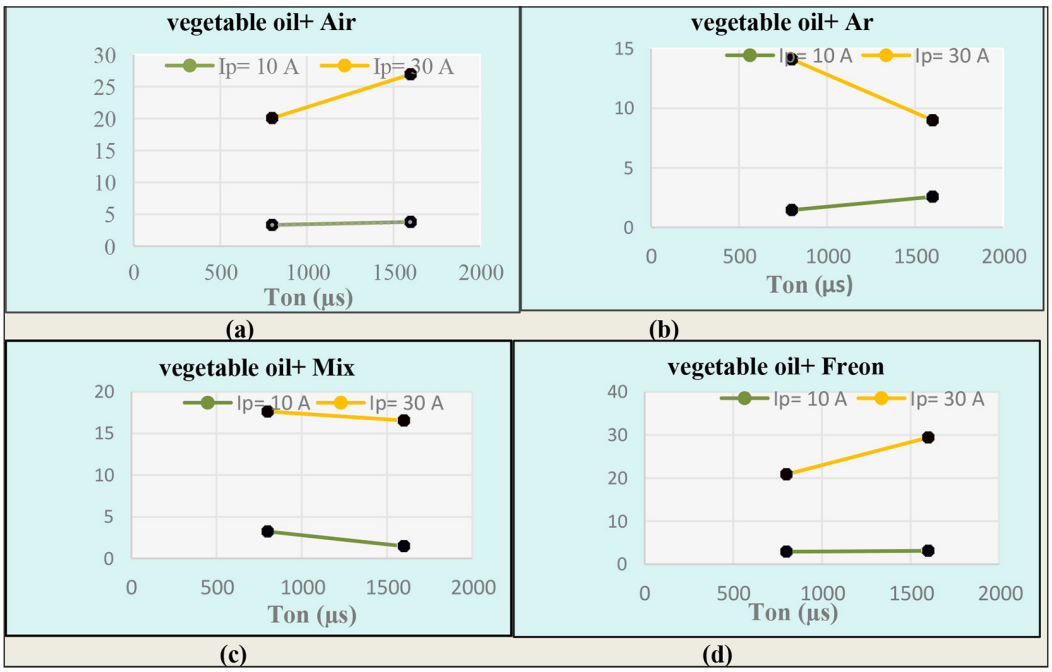

Fig. 2. The effect of Ton on MRR at constant Ip (a) Air, (b) Ar, (c) Mix, and (d) Freon

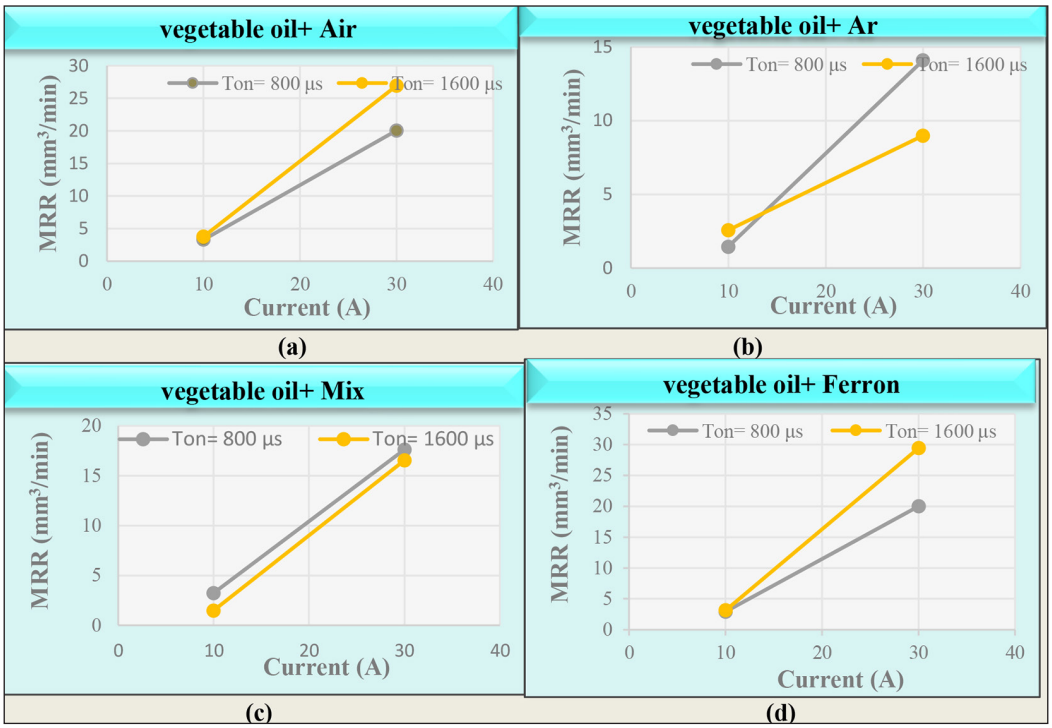

Fig. 3. The effect of Ip on MRR at constant T_{on} (a) Air, (b) Ar, (c) Mix, and (d) Freon

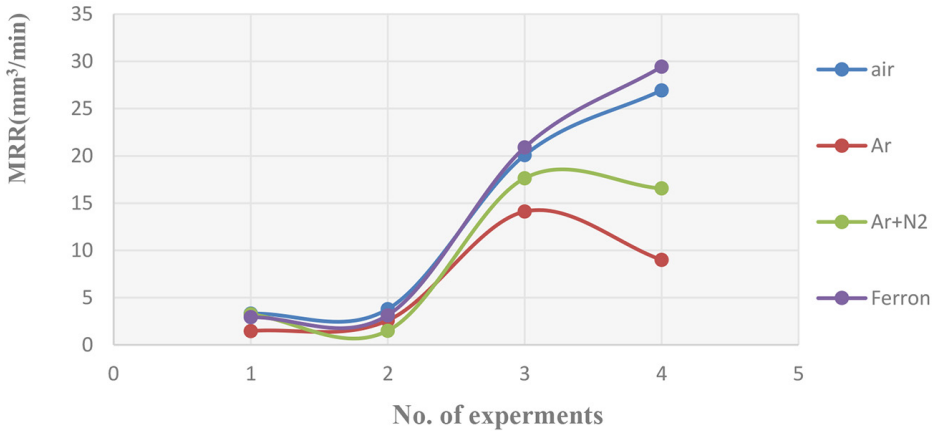

Fig. 4. MRR for ND-EDM experiments

raised the total discharge energy. The high discharge energy melted as well as vaporized further quantity of the material of workpiece, resulting in a bigger size of crater, which resulted in higher MRR. And, this result agrees with Dhakar and Dvivedi 2016 and Singh et al. 2017 [28-29]. ND-EDM improves the flushing efficiency with the help of a high-velocity gas, therefore, MRR increased with an increase in the current.

The increase in pulse on duration time from 800 µs to 1600 µs has been worked on increased the discharge duration time, which effects upon the augmented the discharge energy [30]. Also, the higher discharge energy in the ND-EDM caused the melting as well as the vaporization of further material in the melted puddle and therefore augmented the MRR. Such result agrees with Bai et al. 2013 [31]. When using the Freon mixed gas dielectric, it can be noted that when the pulse on time was increased, the MRR increased slightly and then decreased, as evinced in Figure 2 (d). And, the uppermost MRR at current (30 A) and pulse-on-time (1600) was achieved when using the vegetable oil + Freon gas, and it reached 29.425 mm^3/min and then 26.943 mm^3/min when utilizing the vegetable oil + Air as a dielectric, as illustrated in Figure 4.

The effect of discharge current on the EWR is shown in Figure 5. For the case of the vegetable oil mixed with air, mix, and Freon dielectrics, the EWR values decreased with an increase in the current from 10 A to 30 A, by 211.85% and 140.10% using vegetable oil + Air dielectric, the EWR values increased with an increase in the current, by 250.00% and 140.44 % using vegetable oil + Ar, 359.52% and 68.68% for using vegetable oil + mix (Ar+N_2), and -73.14% (reduction) and 190.18% using vegetable oil + Freon gas, when the used pulse-on-times values were 800 µs and 1600 µs, respectively. Figure 6 (a to d) portrays that the EWR also increased with an increase in the used T_{on} from 800 µs to 1600 µs, i.e., by -9.91% (reduction) and 31.21% using vegetable oil + Air dielectric, 275.00% and 157.62% using vegetable oil + Ar, 30.38% and 40.58% (reduction) using vegetable oil + mix (Ar+N_2), and -17.90% (reduction) and 345.71% using vegetable oil + Freon gas, when the used pulse current values were 10 A and 30 A, respectively.

The reason is increasing the plasma channel which helps in diminishing the short circuiting between the tool and workpiece electrodes. This absence of abnormal discharges or reduced short circuiting improves the heat dissipation and the amount of heat transferred to the too electrode gets reduced to a lower level. This phenomenon of reduced heat transfer brings down the temperature of the materials below melting point and therefore the EWR gets diminished. However, in the case of the (Vegetable oil + Ar), (Vegetable oil + mix (Ar+N_2)), and (Vegetable oil + Freon gas), EWR increase with an increase in current, It can be attributed that higher current produces higher heat density. Thus, it results in erosion of material from tool electrode. At a constant pulse-on-time values of 1600 µs and an increase in the current from 10 A to 30 A, the EWR values were increased in all cases, except for the vegetable oil + Air or feron. The magnitude of EWR was decreased with the increment in the pulse on time ratio's value from 800 µs to 1600 µs while keeping the current constant at 10 A when using the vegetable oil + Argon or Freon as a dielectric, as demonstrated in Figure 6.

This can be attributed to the fact that the used noble gases will isolate the discharge area

from the surrounding air and oxygen in particular, which will reduce the discharge energy and thus obtain the lower wear of electrode. And, this is also owing to the effect of the carbon layer precipitate that's collected upon the surface of electrode, where the deposited layer becomes thicker with the rise in the T_{on} duration. Such layer of carbon works as a wear-resistant layer for electrode as well as helps reduce its wear. And, another cause that participates to the EWR dropping

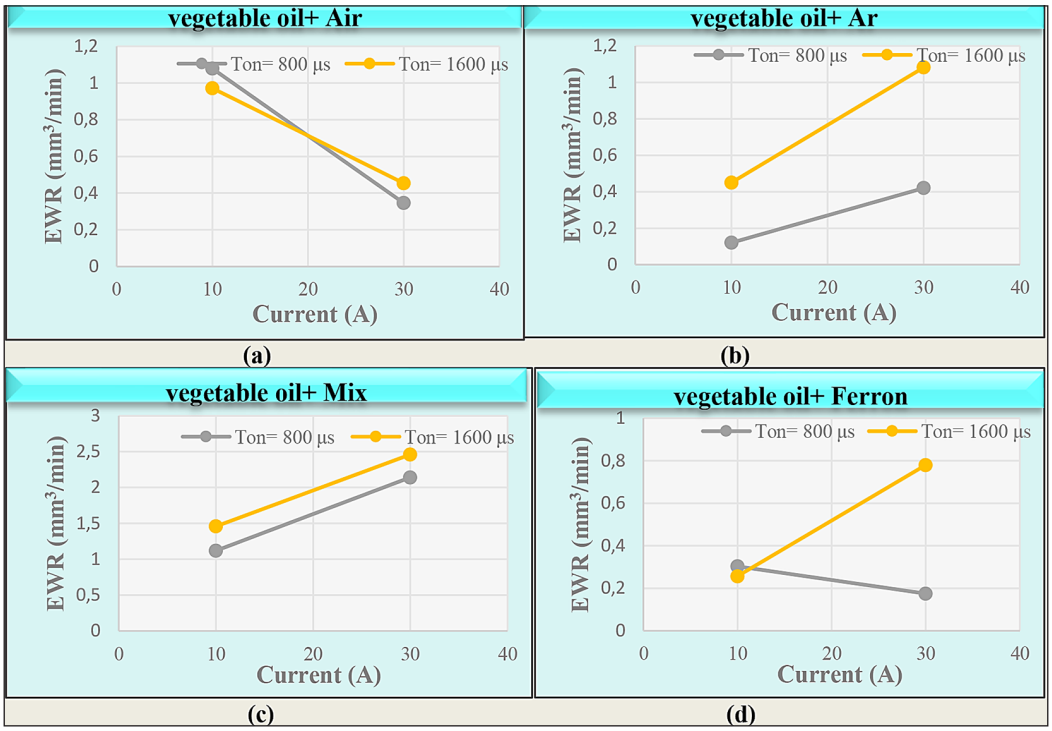

Fig. 5. The effect of T_{on} on EWR at constant I_P (a) Air, (b) Ar, (c) Mix, and (d) Freon

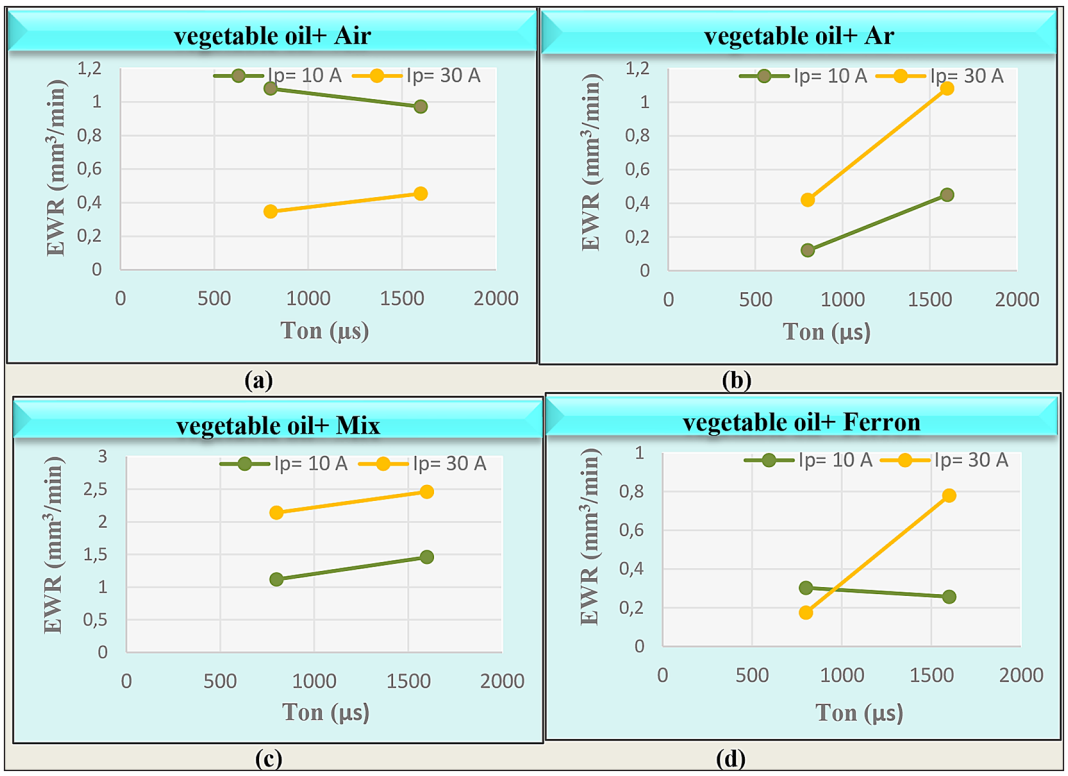

Fig. 6. The effect of I_P on EWR at constant T_{on} (a) Air, (b) Ar, (c) Mix, and (d) Freon

is the plasma channel's expansion at bigger pulse-on-time values. This type of the plasma channel's expansion delays the active heat energy transfer to tool and workpiece also. Because more input heat is practiced via the tool, its wear is markedly decreased. When the pulse current is constant with a value of 30 A, the rise in the pulse-on time magnitude from 800 to 1600 improved the rate of tool wear. And, this is accredited to the cause that an elevated pulse-time ratio means that the spark discharge insists upon a lengthier period. Also, this will produce too much heat input in the tool and in the surface of workpiece, which results in more melting of the electrode and the workpiece; as a result, the EWR was augmented. In addition, this can be ascribed to that the elevated current creates elevated density of heat; therefore, this is what happened as a result of the erosion of material from the tool electrode.

The lowest EWR at the current (10 A) and pulse-on-time (800) was achieved when using the vegetable oil + Argon gas, and it reached 0.120 mm^3/min, and then 0.175 mm^3/min when used at the current (30 A), pulse-on-time (800), and the vegetable oil + Freon gas as a dielectric, as displayed in Figure 7.

The results analysis depicted that the current and pulse-on-time were significant process

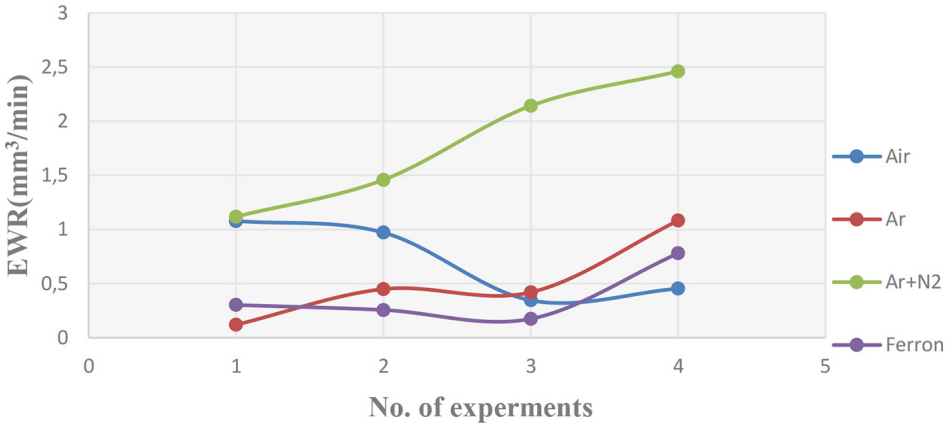

Fig. 7. The EWR for ND-EDM experiments

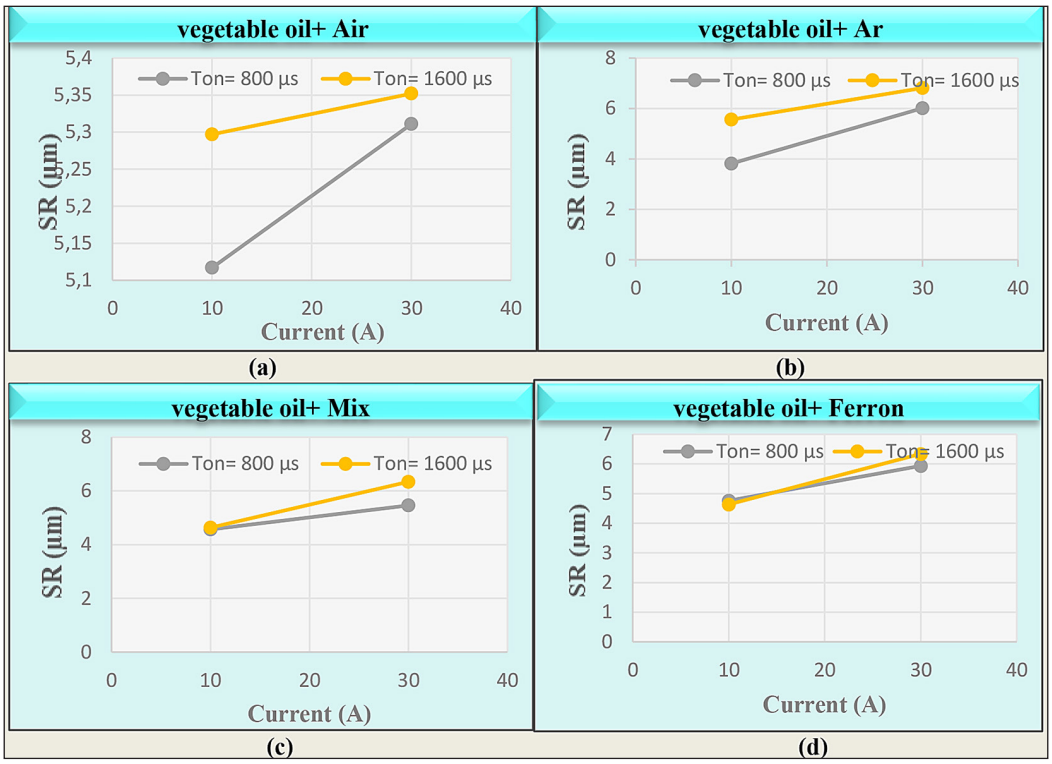

Fig. 8. The effect of I_p on SR at constant T_{on} (a) Air, (b) Ar, (c) Mix, and (d) Freon

parameters for SR in ND-EDM. Figure 8 (a-d) evinces that the SR raised with increasing the current from 10 A to 30 A, by 3.79% and 1.04% using vegetable oil + Air dielectric, 24.70% and 18.71 % using vegetable oil + Ar, 57.63% and 22.50% for ND-EDM (Vegetable oil + mix ($Ar+N_2$)), and 19.58% and 36.84% using vegetable oil + Freon gas, when the used pulse-on-times values were 800 µs and 1600 µs, respectively. This figure shows that the SR also increased or decreased with increased the used T_{on} from 800 µs to 1600 µs, i.e., by 3.52% and 0.79% using vegetable oil + Air dielectric, 11.05% and 5.71 % using vegetable oil + Ar, 45.81% and 13.31% (reduction) using vegetable oil + mix ($Ar+N_2$), and 1.47% and 19.29% for using vegetable oil + Freon gas, when the utilized pulse current values were 10 A and 30 A, respectively.

A bigger size of crater was created when the higher pulse current augmented owing to elevated discharge energy that resulted in a rise in the profiles of surface roughness (SR) [32]. The magnitude of SR was increased with the rise in the pulse-on-time ratio from 800 µs to 1600 µs while keeping the current constant as shown in Figure 9 (a-d), owing to an increment in the discharge energy which was provided for a lengthier period. The high discharge energy raised the size of the created crater [33-34], and a bigger crater caused a rougher surface.

At the elevated pulse-on-time, the pulse-off-time was very low, as well as that was inadequate for re-conditioning the inter-electrode gap (IEG). And, the irregular discharges owing to the debris particles buildup were in charge with the elevated drop in the SR. The lowest SR was achieved at the current (10 A) and pulse-on-time (800) when using the vegetable oil + mix ($Ar+N_2$), and it reached 3.814 µm, and then 4.567 µm when utilizing the vegetable oil + Freon gas as a dielectric, as manifested in Figure 10.

The recast layer is a thin white layer created upon the work-piece's machined surface beyond the EDM procedures. It's evolved if the melted material solidifies through the cooling as well as is deposited upon the finished surface. It's created as a result of the melted material that isn't totally flushed away via the dielectric fluid from the inter-electrode gap (IEG) [35-36]. Such recast hard and brittle layer changes the work material's metallurgical characteristics, which may result in catastrophic failure [37-38]. Therefore, for investigating the different dielectric mediums influence upon the topology of surface, characteristic machined surfaces were examined for the recast layer thickness at higher discharge energy levels. It was observed from the scanning electron microscope (SEM) examination that in the ND-EDM, the average of the recast white layer thickness in

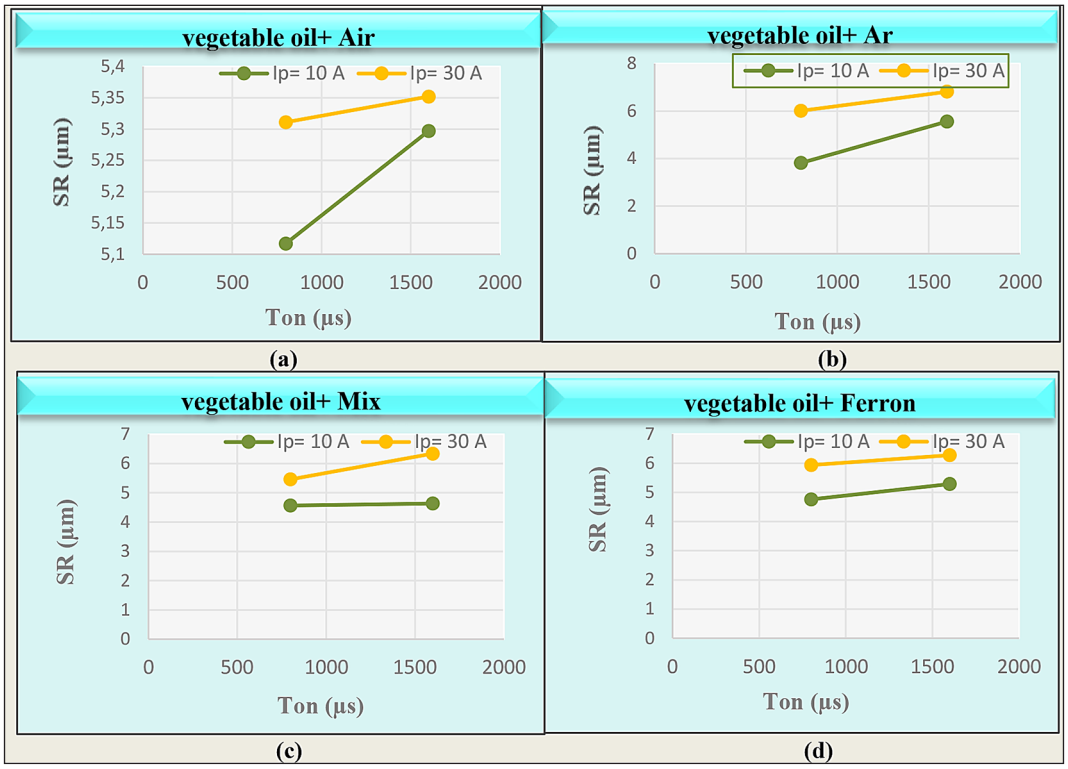

Fig. 9. Effect of the Ton upon the SR at constant Ip (a) Air, (b) Ar, (c) Mix, and (d) Freon

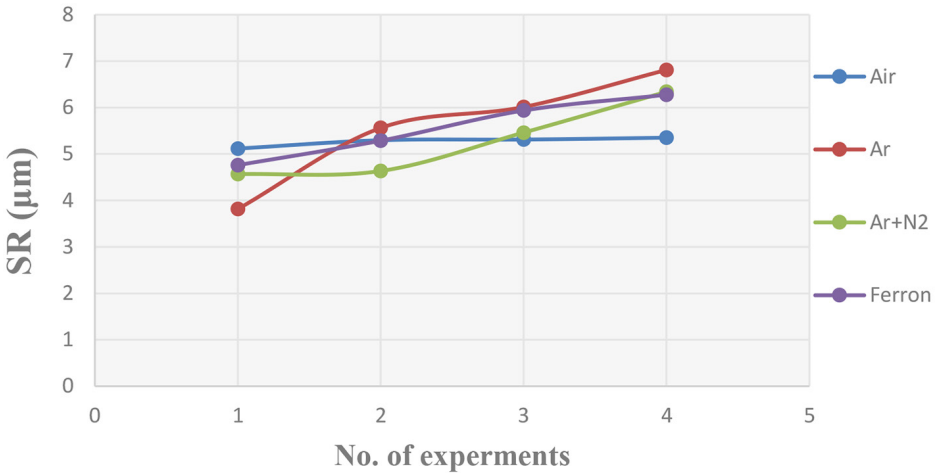

Fig. 10. SR for ND-EDM experiments

the case of vegetable oil + air, Ar, mix (Ar-N_2), and Freon was 1.505, 1.180, 0.456, and 0.000 µm, respectively, as evinced in Figure 11. Freon as gas in ND-EDM didn't create any measurable recast layer thicknesses, and this can be referred to that the vegetable oil + Freon as a dielectric medium makes an explosive reaction between the IEGs spreading out debris from the IEG, therefore, enhancing the flushing efficacy at this gap and subsequently removing the deposition of debris upon the finished surface. And, a thick recast white layer was created via previous traditional EDM at a pulse current of (15 A), which is equal to 31.34 µm [8].

These unique results can be used to increase the service and fatigue life of parts and machines that are exposed to sudden dynamic mechanical or

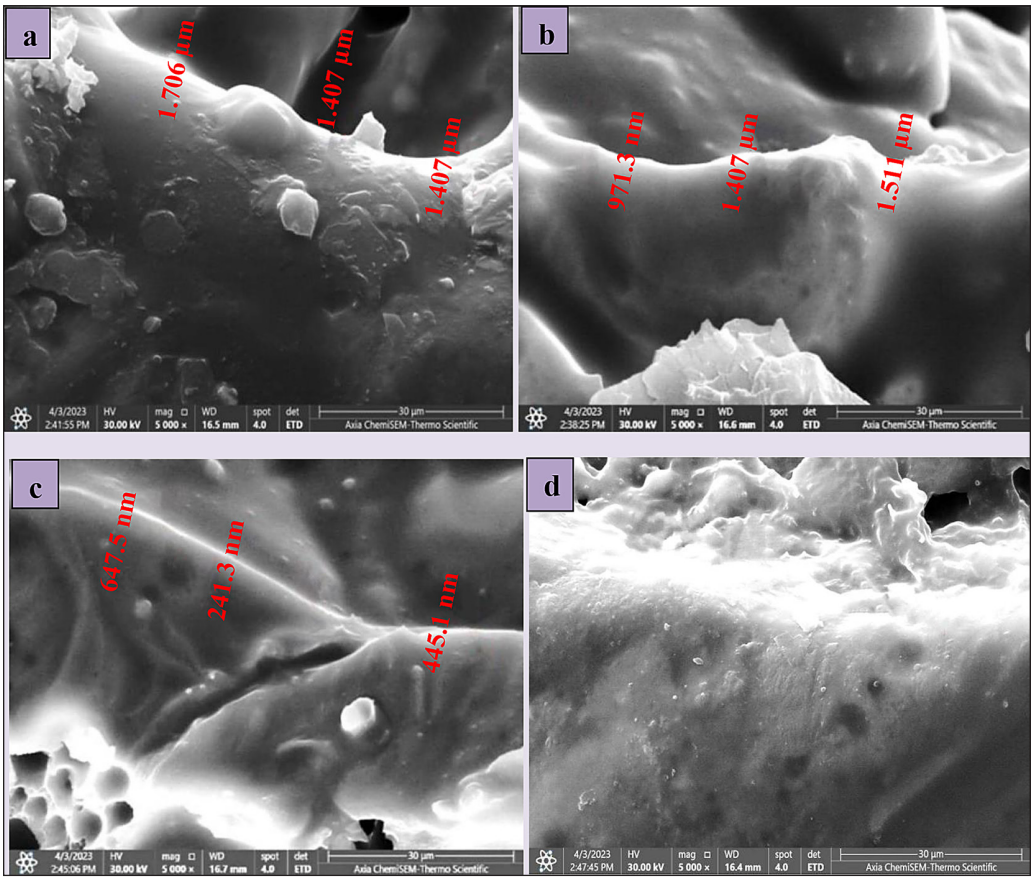

Fig. 11. The SEM examination of the recast white layer thickness for ND-EDM at Ip (30A) and T_{on} (1600 µs); (a) air; (b) Ar; (c) Mix (Ar-N_2); (d) Freon

thermal loads, without the need for additional operations to remove this brittle layer, which causes the failure of these parts with a short service life.

Also, it was experimentally envisaged that among the various additive gases combinations, the dielectric mix with air gas caused the accomplishment of the uppermost MRR. And, the cause ascribed to that the content of O_2 in the air generates more heat through an exothermic reaction and so increases MRR. Such exothermic reactions are in charge with the oxygen content of oxidation [39]. Also, another truth that can either be ascribed to such phenomenon is that O_2 possesses comparatively lower ionization energy in comparison with another gas. Additionally, the gas having lower ionization energy possesses a trend for ionizing further rapidly, which causes elevated obtained MRR [40]. Whereas, owing to the O_2 gas's easy ionization, the atom of O_2 arrests the electrons easily and combines them with positive ions. This easy phenomenon of deionization creates a steady discharge in the situation of O_2-assisted EDM and as a result causes elevated MRR [41]. Furthermore, the flushing of debris by oil-air mixture as a dielectric medium was done better, so the possibility of occurring arc pulses was reduced and so MRR productivity.

The highest achieved MRR by using the input parameters Ip (30A), Ton (1600 µsec), and vegetable oil + Freon as a dielectric reached 29.425 mm^3/min, 26.943 mm^3/min utilizing vegetable oil + Air, 17.626 mm^3/min using mix (Ar+N_2) additive gases to dielectric + 800 µsec, and 14.101 mm^3/min using (Ar additive gas + 800 µsec), as illustrated in Figs. 12 (a).

The comparison of the obtained EWR results for the ND-EDM is demonstrated in Fig. 12 (b). At higher discharge energy levels such as (Ip = 30, Ton = 1600 µs) the enlarged inter-electrode gap (IEG) was in charge with the raising the channel of plasma which aids in lessening the short-circuiting between the workpiece and the tool electrodes. Such nonexistence of irregular discharges or decreased short-circuiting is going to enhance the dissipation of heat, as well as the heat transferred quantity to the two electrodes gets decreased to a lower level.

The lowest achieved EWR that obtained by employing the input parameters Ip (10, 30 A), Ton (800, 1600 µsec), and vegetable oil with

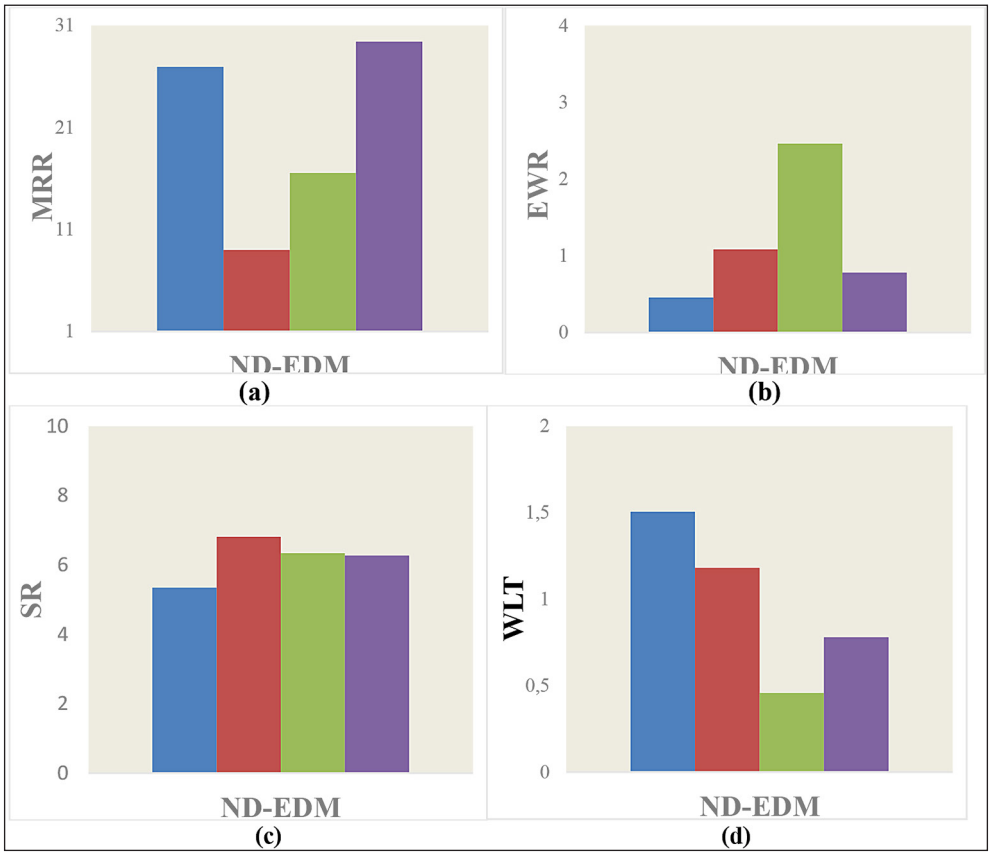

Fig. 12. The performance results of ND-EDM experiments; (a) MRR; (b) EWR; (c) SR; (d) The white recast layer thickness

Air, Ar, mix (Ar+N_2) and Freon additive gases reached 0.346 mm^3/min (using 800 µsec, 30A), 0.120 (used 800 µsec, 10A), 1.119 (utilizing 800 µsec, 10A), and 0.175 (using 800 µsec, 30A), respectively, as shown in Fig. 12 (b).

The comparison of obtained SR for the ND-EDM is demonstrated in 12 (c). The lowest achieved SR by using (10 A, Ton 800 µsec) and the additive Air, Ar, mix (Ar +N_2), and Freon gases to dielectric reached, 5.117 µm, 4.76 µm 1, 3.814, and 4.567 µm, respectively, and the lowest SR values obtained for all the designed experiments reached 3.287 µm when using Ip (10 A), Ton (1600 µsec), and Ar additive gas, followed by 4.567 µm when adding Freon gases to the dielectric.

The comparison of the obtained white recast layer (RL) thickness for the ND-EDM, is demonstrated in Fig. 12 (d). At the higher discharge energy levels such as (Ip = 30, Ton = 1600 µs,). The RL thickness value was received in vegetable oil-Freon (ND-EDM), its minimum values and didn't create any measurable recast layer. It can be attributed that the vegetable oil-Freon as a dielectric medium creates an explosive reaction between the inter electrodes gaps (IEGs) spreading out debris from this gap, therefore, enhancing flushing efficacy at the IEG and as a result eliminates the deposition of debris on the finished surface. The RL thickness obtained by using the air as a dielectric medium in any method was almost (4) times larger than the else dielectric mediums.

The current experimentation purpose is to generate statistical models for ND-EDM and plots for determining the effect of using different dielectric mixtures performed by using the 2^2 (level ^{factor}) Full Factorial Design (FFD). And, the (2) chosen parameters for the EDM experiments are the controllable factors having a chief part to take in the procedure description, including the pulse current with two numeric levels of (10 A and 30 A) as well as pulse-on-time with (2) numeric levels of (800 µm and 1600 µm) and one for no. of replicates. Also, the overall FFD with a (95%) confidence interval scrutinizes the investigated values that were implemented via using the Minitab statistical software with the overall linear model.

The coefficients of determination were used to develop the mathematical model and predict the procedure responses for ND-EDM utilizing the investigational outcomes determined from Tables 10. The equations from (1) to (3) elucidate the regression models in un-coded form, which connect between the procedure factors as well as the responses of material removal rate (MRR), electrode wear rate (EWR), and surface roughness (SR), correspondingly.

$$\mathrm{MRR} = -0.0180 + 0.002750\ \mathrm{Ip} \quad (1)$$

$$\mathrm{EWR} = 0.011000 - 0.000250\ \mathrm{Ip} \quad (2)$$

$$\mathrm{SR} = -5.139 + 0.00640\ \mathrm{Ip} \quad (3)$$

The plots of normal probability of residuals for MRR, EWR, and SR using the experimental results obtained from Table 6 are shown in Figure 13 (a to c) for ND-EDM (air +vegetable oil), respectively. And, they reveal a clear pattern (that means the points have been steadied in a straight line) indicating that every parameter influences the MRR, EWR, and SR in the ND-EDM as well as their outcomes from the regression model (predicted value via FFD) and true values (from the experiments).

The regression coefficients were utilized for developing the mathematical model as well as predicting the process responses for ND-EDM with (Ar +vegetable oil) dielectric employing the investigational outcomes determined from the Table 7. The equations from (4) to (6) demonstrate the regression models in the un-coded form, which connect between the procedure factors and the responses of material removal rate (MRR), electrode wear rate (EWR), and surface roughness (SR), correspondingly.

$$\mathrm{MRR} = -0.00800 + 0.002050\ \mathrm{Ip} - 0.000005\ \mathrm{Ton} \quad (4)$$

$$\mathrm{EWR} = 0.000025 - 0.000007\ \mathrm{Ip} \quad (5)$$

$$\mathrm{SR} = 1.915 + 0.0862\ \mathrm{Ip} + 0.001592\ \mathrm{Ton} \quad (6)$$

Plots of the residuals normal probability for the MRR, EWR, and SR are depicted in the Figure 14 (a-c) for ND-EDM with (Ar +vegetable

Table 12. Values of the experimented and predicted responses for ND-EDM (air + vegetable oil)

Run order	Exp. MRR g/min	Pred. MRR g/min	Residual value	Exp. EWR (g/min)	Pred. EWR (g/min)	Residual value	Exp. SR (µm)	Pred. SR (µm)	Residual value
1	0.0092	0.009	-0.000	$9.647*10^{-3}$	0.003	0.000	5.110	5.203	0.093
2	0.0105	0.009	0.000	$8.609*10^{-3}$	0.008	0.000	5.297	5.203	-0.093
3	0.0556	0.064	0.009	$3.092*10^{-3}$	0.003	-0.000	5.311	5.331	-0.020
4	0.0749	0.064	-0.009	$4.059*10^{-3}$	0.008	0.000	5.352	5.331	0.020

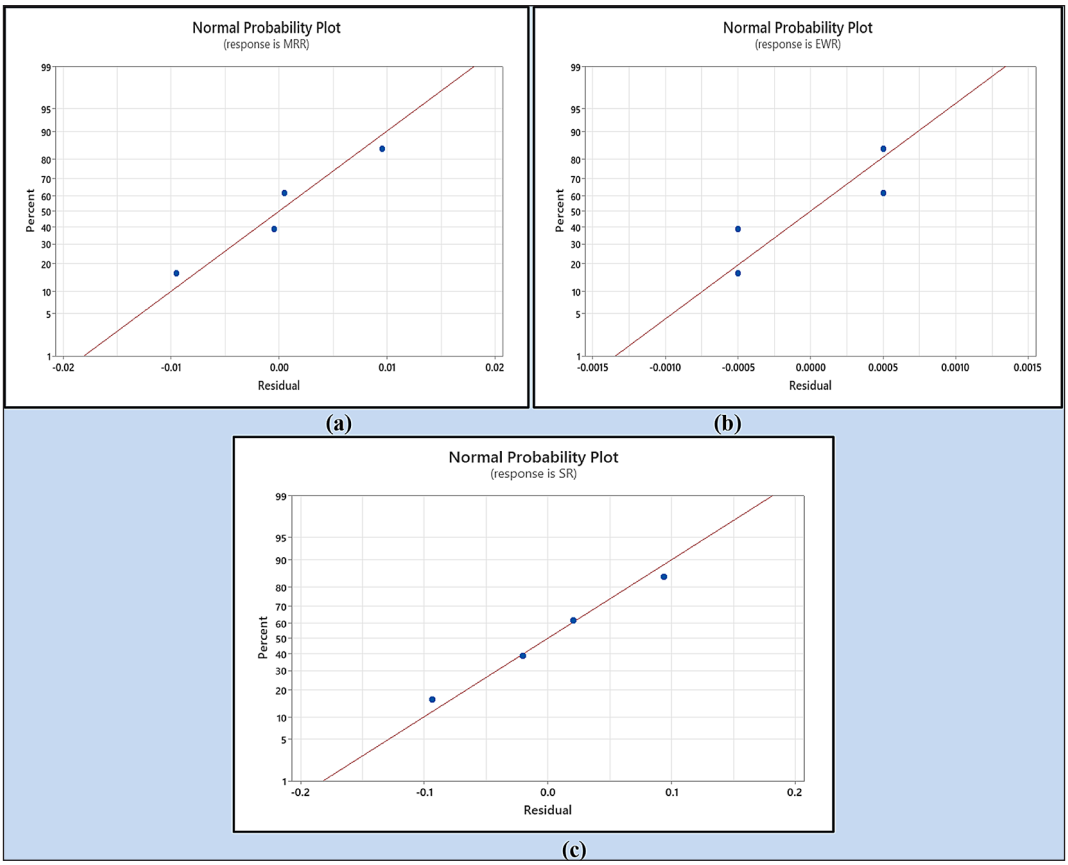

Fig. 13. The normal probability plots of residuals for ND-EDM (air +vegetable oil) (a) MRR, (b) EWR, (c) and SR

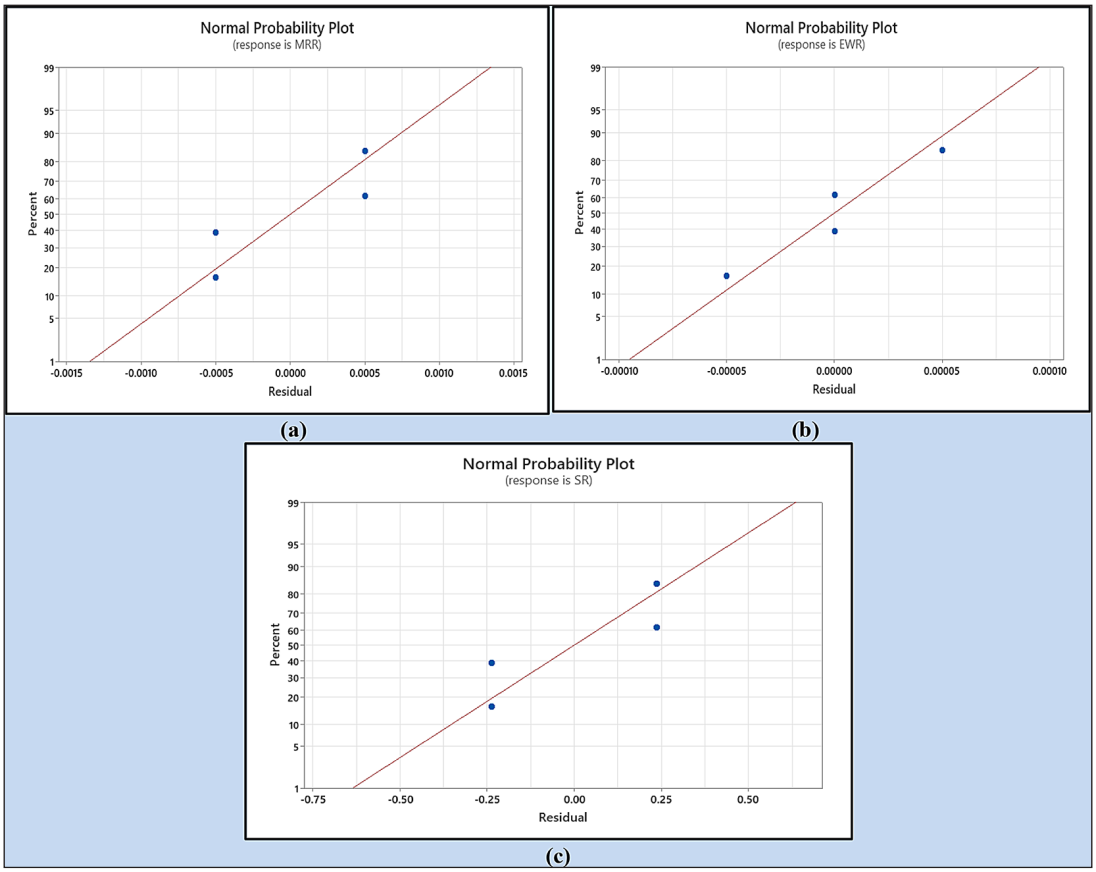

Fig. 14. The normal probability plots of residuals for ND-EDM (Ar +vegetable oil); (a) MRR, (b) EWR, (c) and SR

oil) dielectric, respectively. And, they portray a clear pattern (that means the points have been steadied in a straight line) indicating that every parameter influences the MRR, EWR, and SR in the ND-EDM as well as their outcomes from the regression model (predicted value via FFD) and true values (from the experiments).

The regression model coefficients were employed for developing the mathematical model and predicting the process responses for ND-EDM with (Mix (Ar+N_2) + vegetable oil) dielectric utilizing the investigational outcomes determined from the Table 8. The equations from (7) to (9) manifest the regression models in the un-coded form, which connect between the procedure factors and the responses of material removal rate (MRR), electrode wear rate (EWR), and surface roughness (SR), correspondingly.

$$MRR = -0.0220 + 0.003000\ Ip \quad (7)$$

$$EWR = 0.00050 - 0.000001\ Ip \quad (8)$$

$$SR = 3.950 + 0.0650\ Ip \quad (9)$$

Plots of the residuals normal probability for the MRR, EWR, and SR are evinced in Figure 15 (a-c)) for ND-EDM with (Mix (Ar+ N_2) + vegetable oil) dielectric, respectively. And, they illustrate a clear pattern (that means the points have been steadied in a straight line) indicating that every parameter influences the MRR, EWR, and SR in the ND-EDM as well as their outcomes from the regression model (predicted value via FFD) and true values (from the experiments).

The regression model coefficients were employed to developing the mathematical model and predicting the process responses for ND-EDM with (Freon + vegetable oil) dielectric utilizing the investigational outcomes determined from the Table 9. The equations from (10) to (12) display the regression models in the un-coded form, which connect between the procedure factors and the responses of material removal rate (MRR), electrode wear rate (EWR), and surface roughness (SR), correspondingly.

$$MRR = -0.00775 + 0.001325\ Ip \quad (10)$$

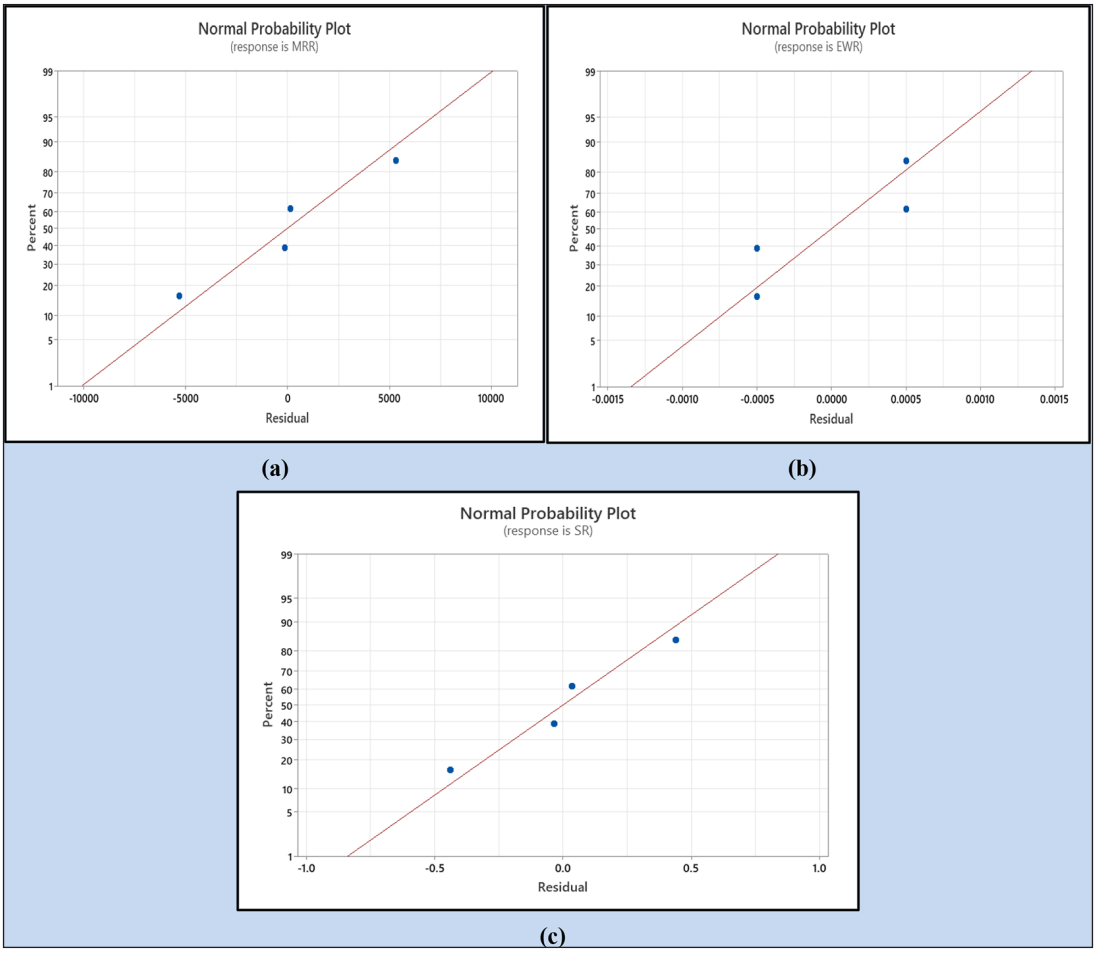

Fig. 15. The normal probability plots of residuals for ND-EDM (Mix (Ar+N_2) + vegetable oil); (a) MRR, (b) EWR, (c) and SR

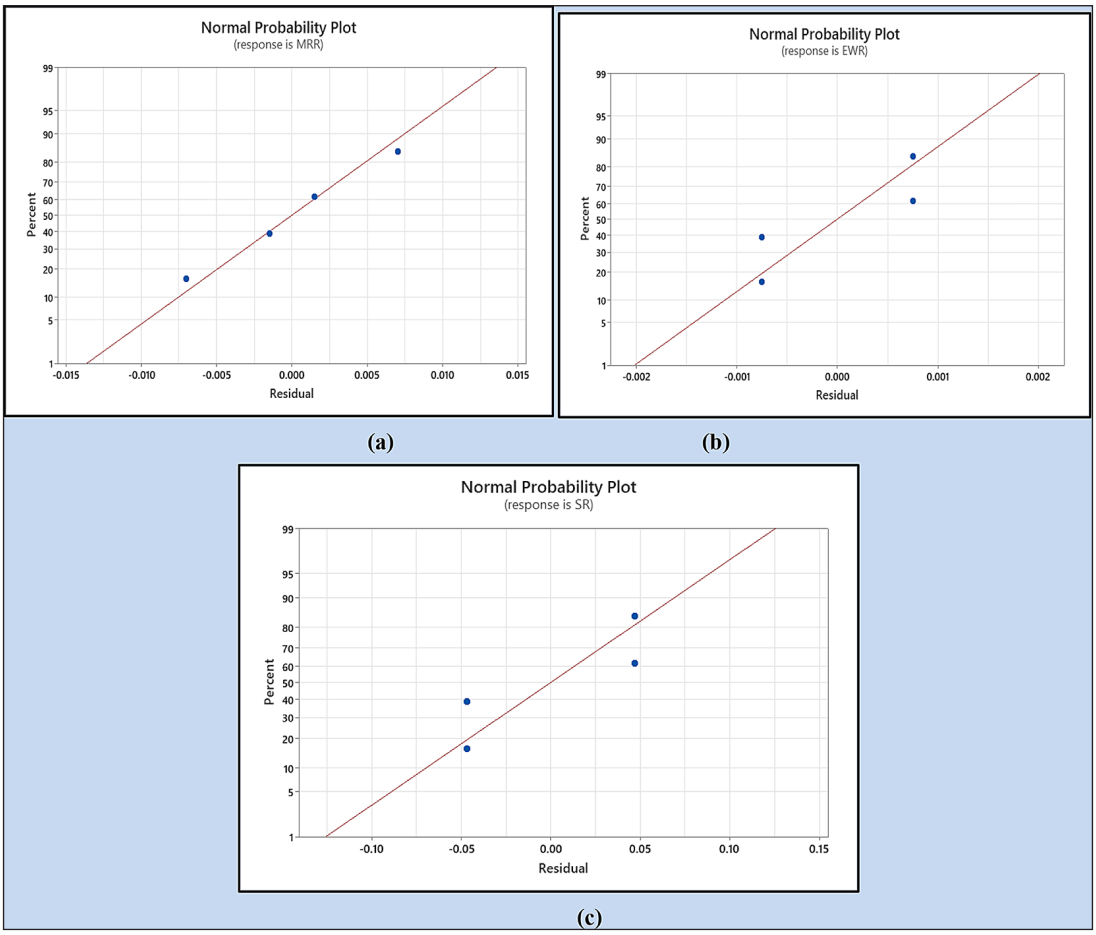

Fig. 16. The normal probability plots of residuals for ND-EDM (Freon+ vegetable oil); (a) MRR, (b) EWR, (c) and SR

$$EWR = -0.00600 + 0.000175\ Ip + 0.000006\ Ton \quad (11)$$

$$SR = 3.834 + 0.05412\ Ip + 0.000541\ Ton \quad (12)$$

Plots of the residuals normal probability for the MRR, EWR, and SR are exhibited in Figure 16 (a-c) for ND-EDM with (Freon + vegetable oil), respectively. And, they indicated a clear pattern (that means the points have been steadied in a straight line) indicating that every parameter influences the MRR, EWR, and SR in the ND-EDM as well as their outcomes from the regression model (predicted value via FDD) and true values (from the experiments).

CONCLUSIONS

The main conclusions of the current work can be summarized in the following. In the near-dry EDM, the highest MRR achieved when using (Vegetable oil + Freon gas), reached 29.425 mm^3/min, and then 26.943 mm^3/min when using Vegetable oil + Air as a dielectric. Compared to the gases used in the ND-EDM, it found that the highest MRR was achieved when using the (Vegetable oil + Freon gas, Air and Mix (Ar+N_2) produced 227.199%, 199.6%, and 83.999% higher than using the (Vegetable oil + Ar) at higher I_p (30 A), higher value of T_{on} (1600 µs), respectively. In the near-dry EDM, the lowest EWR produced was achieved reached 0.120 mm^3/min, and then 0.175 mm^3/min when used a pulse current (10A) and (30A) and Pulse-on-time (800) and the Vegetable oil + Freon gas as a dielectric. Compared to the gases used in the ND-EDM, it is found the EWR in (Vegetable oil + Air, Freon and then with Ar) produced 81.552%, 68.306%, and 56.034% lowest EWR, respectively, than (Vegetable oil + Mix (Ar+N_2)) at higher I_p (30 A), and higher value of T_{on} (1600 µs). The lowest SR was achieved at current (10A) and Pulse-on-time (800) when using the ND-EDM (Vegetable oil + mix (Ar+ N_2)), reached 3.814 µm, and then 4.567 µm when using the Vegetable oil + Freon gas. Compared to

the gases used in the ND-EDM, it found SR in (Vegetable oil + Air, Freon, Mix(Ar+N_2)) produced 13.43%, 2.60%, and 1.45% lowest SR, respectively, than (Vegetable oil +Ar) at higher I_p (30 A), and higher value of T_{on} (1600 μs). In the ND-EDM, the average of recast white layer thickness in the case of vegetable oil + air, vegetable oil + Ar, vegetable oil + mix (Ar-N_2), and vegetable oil + Freon were 1.50 μm 5, 1.180 μm, 0.456 μm, and 0.000 μm, respectively. The lowest obtained white recast layer (WLT) thickness value was achieved and did not produce any measurable recast layer when adding Freon during the (ND-EDM). These unique results can be used to increase the service and fatigue life of parts and machines that are exposed to sudden dynamic mechanical or thermal loads, without the need for additional operations to remove this brittle layer, which causes the failure of these parts with a short service life. The created mathematical models displayed a higher value of R-Square and the adjusted R-square, which indicates a better fit. The plots of normal probability of residuals for MRR, EWR, and SR elucidated an obvious pattern (i.e., the points have been stabilized in a straight line) which indicates that each factor affects the mentioned responses and the results of these responses from the regression model (predicted value by the factorial) and the true values (from the experiments).

REFERENCES

1. Rajurkar K.P., Sundaram M.M., Malshe A.P. Review of Electrochemical and Electrodischarge Machining. Procedia CIRP 2013; 6: 13–26. doi:10.1016/j.procir.2013.03.002.
2. Abbas N.M., Solomon D.G., Bahari M.F. 2007. A review on current research trends in electrical discharge machining (EDM). International Journal of Machine Tools and Manufacture, 47: 1214–1228.
3. Pandey A., Singh S. 2010. Current research trends in variants of Electrical Discharge Machining: A review. International Journal of Engineering Science and Technology. 2010; 2: 2172–2191.
4. Grzesik W. 2008. Advanced machining processes of metallic materials: theory, modelling and applications. Elsevier.
5. Groover M.P. Fundamentals of modern manufacturing: materials processes, and systems. John Wiley & Sons. 2007.
6. Ali S.M. Influence of Electrodes and Parameters on Micro-EDM Drilling Performances of 304L Stainless Steel" 2nd International Iraqi Conference on Engineering Technology and its Applications (2ndIICETA), 27–28, August 2019, Proceedings of the IEEE Xplore, 1–6, 2020.
7. Paramashivan S.S., Mathew J., Mahadevan S. 2012. Mathematical modeling of aerosol emission from die sinking electrical discharge machining process. Applied Mathematical Modelling. 2012; 36: 1493–1503.
8. Abrol A., Singla V.K. Study on Optimization and Machining Characteristics of Electric Discharge Machining Using Powder Suspension Dielectric Fluids. Thapar University. 2013.
9. Abukhshim N.A., Mativenga P.T., Sheikh M.A. Heat generation and temperature prediction in metal cutting: A review and implications for high speed machining. International Journal of Machine Tools and Manufacture. 2006; 46: 782–800.
10. Al-Khazraji A., Amin S., Ali S.M. The Effect of SiC powder Mixing Electrical Discharge Machining (PMEDM) on Fatigue Life of AISI D2 Die Steel", Engineering Science and Technology, an International Journal. 2016; 19: 1400–1415.
11. Shivakoti I., Kibria G., Diyaley S., Pradhan B.B. Multi-objective optimization and analysis of electrical discharge machining process during micro-hole machining of D3 die steel employing salt mixed deionized water dielectric. Journal of Computational & Applied Research in Mechanical Engineering. 2013; 3: 27–39.
12. Jose M., Sivapirakasam S.P., Surianarayanan M. 2010. Analysis of aerosol emission and hazard evaluation of electrical discharge machining (EDM) process. Industrial Health: 48: 478–486.
13. Goh, C.L., Ho, S.F. Contact Dermatitis from Dielectric Fluids in Electrodischarge Machining. Contact Dermatitis. 1993; 28(3): 134–138. DOI: 10.1111/j.1600-0536.1993.tb03372.x.
14. Al-Khazraji B.A., Amin S., Ali S.M. Fatigue Life of Graphite Powder Mixing Electrical Discharge Machining AISI D2 Tool Steel. Journal of Solid Mechanics. 2018; 10(2): 338–353.
15. Singh N.K., Pandey P.M., Singh K.K., Sharma M.K. Steps Towards Green Manufacturing through EDM Process: A Review. Cogent Eng. 2016; 3(1): 1–13. DOI: 10.1080/23311916.2016.1272662.
16. Kumar A., Maheshwari S., Sharma C., Beri N. Research Developments in Additives Mixed Electrical Discharge Machining (AEDM): A State of Art Review. Mater. Manuf. Process. 2010; 25(10): 1166–1180. DOI: 10.1080/10426914.2010.502954
17. Dhakar K., Dvivedi A. Dry and Near-Dry Electric Discharge Machining Processes, In Advanced Manufacturing Technologies. Materials Forming, Machining and Tribology; Gupta, K. Eds; Springer: Cham. 2017; 249–266.

18. Nimbalkar V.S., Shete P.M.T. Experimental Investigation of Machining Parameters Using Solid and Hollow Electrode for EDM of Ti-6Al-4V. Int. Res. J. Eng. Technol. 2017; 4: 2345.
19. Wang X.; Yi S.; Guo H.; Li C.; Ding S. Erosion Characteristics of Electrical Discharge Machining Using Graphene Powder in Deionized Water as Dielectric. Int. J. Adv. Manuf. Technol. 2020; 108: 357–368. [CrossRef]
20. Jahan M.P., Kakavand P., Alavi F. A Comparative Study on Micro-Electro-Discharge-Machined Surface Characteristics of Ni-Ti and Ti-6Al-4V with Respect to Biocompatibility. Procedia Manuf. 2017; 10: 232–242. [CrossRef]
21. Rahman M., Wang Z.G., Wong, Y.S. A Review on High-Speed Machining of Titanium Alloys. In Proceedings of the 3rd International Conference on Leading Edge Manufacturing in 21st Century, Nagoya, Japan, 19–22 October 2005; 49: 19–28.
22. Hocheng H., Tsai H.Y. Advanced Analysis of Nontraditional Machining; Springer Science & Business Media: Berlin/Heidelberg, Germany, 2013.
23. Alidoosti A., Ghafari-Nazari A., Moztarzadeh F., Jalali N., Moztarzadeh S., Mozafari M. Electrical Discharge Machining Characteristics of Nickel-Titanium Shape Memory Alloy Based on Full Factorial Design. J. Intell. Mater. Syst. Struct. 2013; 24: 1546–1556. [CrossRef]
24. Chen S.L., Hsieh S.F., Lin H.C., Lin M.H., Huang J.S. Electrical Discharge Machining of TiNiCr and TiNiZr Ternary Shape Memory Alloys. Mater. Sci. Eng. A. 2007; 445–446: 486–492. [CrossRef]
25. Sahin Y., Murphy S. The effect of fiber orientation of the dry sliding wear of borsic reinforced aluminum alloy. Journal of materials science. 1996; 31: 5399–5407.
26. Amirkhanlou S., Niroumand B. Synthesis and Characterization of 356-SiCp composites by Stir casting and compocasting methods, Trans. Nonferrous. Met. Soc. China. 2010; 20: 788–793.
27. Dhakar K.; Dvivedi A. Parametric Evaluation on Near-Dry Electric Discharge Machining. Mater. Manuf. Process. 2016; 31(4): 413–421. DOI: 10.1080/10426914.2015.1037905.
28. Singh N.K., Pandey P.M., Singh K.K. Experimental Investigations into the Performance of EDM Using Argon Gas-Assisted Perforated Electrodes. Mater. Manuf. Process. 2017; 32(9): 940–951. DOI: 10.1080/10426914.2016.1221079.
29. Gupta P.K., Dvivedi A., Kumar P. Effect of Pulse Duration on Quality Characteristics of Blind Hole Drilled in Glass by ECDM. Mater. Manuf. Process. 2016; 31(13): 1740–1748. DOI: 10.1080/10426914.2015.1103857.
30. Bai X., Zhang Q.H., Yang T.Y., Zhang J.H. Research on Material Removal Rate of Powder Mixed near Dry Electrical Discharge Machining. Int. J. Adv. Manuf. Technol. 2013(68); 1757–1766.
31. Upadhyay L., Aggrawal M.L., Pandey P.M. Performance Analysis of Magnetorheological Fluid-Assisted Electrical Discharge Machining. Mater. Manuf. Process. 2018; 33(11): 1205–1213. DOI: 10.1080/10426914.2017.1364852.
32. Van Dijck F.S., Dutre W.L. Heat Conduction Model for the Calculation of the Volume of Molten Metal in Electric Discharges. J. Phys. D. Appl. Phys. 1994; 7: 899–910. DOI: 10.1088/0022-3727/ 7/6/316.
33. Prakash C., Kansal H.K., Pabla, B.S., Puri, S. Experimental Investigations in Powder Mixed Electric Discharge Machining of Ti–35Nb–7Ta–5Zrβ-Titanium Alloy. Mater. Manuf. Process. 2017; 32(3): 274–285. DOI: 10.1080/10426914.2016.1198018.
34. Kruth J.P., Stevens L.L., Froyen B.L., Leuven K.U. Study of the white layer of a surface machined by diesinking electrodischarge machining, Ann. CIRP. 1995; 44(1): 169-172.
35. Pragadish N., Pradeep Kumar M. Surface characteristics analysis of dry EDMed AISI D2 steel using modified tool design, JMST. 2015; 29(4): 1737-1743.
36. Rebelo J.C., Dias A.M., Kremer D., Lebrun J.L. Influence of EDM pulse energy on the surface integrity of martensitic steels, J. of Materials Processing Technology. 1998; 84(1-3): 90-96.
37. Kumar S., Batish A., Singh R., Singh T.P. A hybrid Taguchi-artificial neural network approach to predict surface roughness during electric discharge machining of titanium alloys, JMST, 2014; 28(7): 2831-2844.
38. Kunleda M., Miyoshi Y., Takaya T., et al. High speed 3D milling by dry EDM. CIRP. 2003; 52: 147–150.
39. Li L.Q., Zhao W.S., Di S.C., et al. Experimental study on electrical discharge machining in gas. JME. 2006; 42: 203.
40. Liqing L., Yingjie S. Study of dry EDM with oxygen-mixed and cryogenic cooling approaches. Procedia CIRP. 2013; 6: 344–350.